CONF-9505167--2

LASER-SOLID INTERACTION AND DYNAMICS OF LASER-ABLATED MATERIALS

K. R. Chen, J. N. Leboeuf, R. F. Wood, D. B. Geohegan, J. M. Donato, C. L. Liu, and A. A. Puretzky

Oak Ridge National Laboratory, P. O. Box 2009, Oak Ridge. TN 37831-8071, USA

ABSTRACT

An annealing model is extended to treat the vaporization process, and a hydrodynamic model describes the ablated material. We find that dynamic source and ionization effects accelerate the expansion front of the ablated plume with thermal vaporization temperature. The vaporization process and plume propagation in high background gas pressure are studied.

1. INTRODUCTION

Laser materials processing techniques are expected to have a dramatic impact on materials science and engineering in the near future and beyond. One of the main laser materials processing techniques is Pulsed Laser Deposition (PLD) for thin film growth. While experimentalists search for optimal approaches for thin film growth. a systematic effort is needed in theory and modeling of various processes during PLD. In this paper, we study three physics issues important to PLD: laser-solid interaction, dynamic source effect for an accelerated expansion, and background gas effect on the dynamics of ablated materials.

2. LASER-SOLID INTERACTION

We have extended a laser-annealing model, Laser8 [1], to include the vapor production stage. The model employs a finite-difference method to solve the heat diffusion equation with enthalpy, temperature, and a state diagram. The model can handle phase transitions, which may or may not be in equilibrium, through the state array concept according to the state diagram. For the phase transition from liquid to vapor. the vaporization temperature is determined by the pressure at the liquid surface, P_s, according to the Clausius-Clapeyron

DISCLAIMER

DISCLAIMER

Portions of this document may be illegible in electronic image products. Images are produced from the best available original document.

equation:

$$T_v = [\frac{1}{T_o} - \frac{\ln(P_s/P_o)}{\Delta H}]^{-1}, \quad (1)$$

where T_o is a known reference vaporization temperature at a reference pressure, (P_o), and ΔH is the latent heat for vaporization. Here we assume that the materials emitted from the surface before vaporization (due to other mechanisms such as ionic emission) maintain an equilibrium pressure with the background. In this model the surface pressure is given as a constant for boiling cases or by the surface pressure from the hydrodynamic model.

When the surface pressure is one atmosphere, the corresponding boiling temperature is 3267℃ for silicon. We calculate the interaction of the silicon solid with a 40-ns (FWHM) KrF (248-nm wavelength) laser. Two particuler modeling results give the time history of the surface temperature for the cases of the laser-energy-density. E, which are 3.8 and 3.9 J/cm^2. At 3.8 J/cm^2, the silicon surface never reaches the boiling temperature and no material is vaporized. At 3.9 J/cm^2, it reaches the boiling temperature and a thin layer of silicon about 4.4×10^{-8}cm becomes vapor. Therefore, the laser-energy-density threshold for boiling silicon in air with a KrF laser is about 3.9 J/cm^2. This is consistent with experimental measurements, which show that the silicon surface remains liquid with 1.9 J/cm^2[2] and that visible surface damage by vaporization did not to occur until $E \sim 4.5$ J/cm^2 of XeCl (308-nm wavelength) laser[3].

For the surface pressure at 1 mTorr, the corresponding boiling temperature is 1615℃. From the modeling, we know that the laser-energy-density threshold is about 1.4 J/cm^2. The experimental data of D. B. Geohegan show that his ion probe receives a signal at 1.5 J/cm^2 or higher, and no signal is detected at lower laser energy density. Again, the modeling result has good agreement with experimental measurements.

Figure 1 shows the laser-energy-density threshold and the boiling temperature vs. the surface pressure for silicon. For the surface pressure below 3.1×10^{-5} Torr, the boiling temperature is equal to the melting temperature. There is no liquid phase. Therefore, the solid can directly vaporize. The laser energy density required to reach this temperature is about 0.7J/cm^2. For surface pressures higher than that, the higher the pressure, the

higher the vaporization temperature. Modeling results show that the laser-energy-density threshold is linearly proportional to $\log P_s$. We also know from modeling the amount of material removed for different laser energy densities. Both the maximum speed of surface recession due to vaporization and the depth of vaporization are linearly proportional to the laser energy density above its threshold at different background pressures.

3. DYNAMIC SOURCE EFFECT

The quality of film deposited critically depends on the range and profile of the kinetic energy and density of the ablated plume[4]. Plumes that are too energetic causes film damage. It is well known[5, 6] that the maximum escape velocity of an original stationary gas is $2c_s/(\gamma-1)$ for an unsteady expansion, where c_s is the initial sound speed and γ is the ratio of specific heats. However, experimental measurements always show that at low laser fluence in which the laser energy absorbed by the plume is negligible, the expansion front is two to three times faster than predicted from unsteady adiabatic expansion with typical vaporization temperatures[6].

We have found a dynamic source effect that accelerates the unsteady expansion significantly faster than predicted from conventional models in the direction perpendicular to the target surface. An effect of dynamic partial ionization that increases the expansion in all directions is also studied. As in previous work[6, 7], we are interested in a laser fluence range high enough for hydrodynamic theory to be applicable, but low enough for the absorption of the laser energy by the plume to be weak so that we can compare it with free expansion models that do not include absorption.

In our model the same material is treated as a dynamic source into the system after $t = 0$. For the plume pressure, P, below its thermodynamic critical pressure and with low plume viscosity, we may assume that the plume behaves as an ideal gas such that $P = n(1+\eta)k_BT$, where n (T) is the density (temperature) of the plume, η is the ionization fraction, and k_B is the Boltzmann constant. We use Euler's fluid equations to model the plume dynamics and

the Saha equation to determine the ionization fraction[8]:

$$\frac{\partial}{\partial t}(n) = -\frac{\partial}{\partial x}(nv) + S_n\delta(x - x_s)\,, \tag{2}$$

$$m\frac{\partial}{\partial t}(nv) = -\frac{\partial}{\partial x}(P + mnv^2)\,, \tag{3}$$

$$\frac{\partial}{\partial t}(E) = -\frac{\partial}{\partial x}[v(E + P)] + S_E\delta(x - x_s)\,, \tag{4}$$

$$\frac{\eta^2}{1-\eta} = \frac{2}{n}\frac{u_+}{u_o}\left(\frac{2\pi m_e k_B T}{h^2}\right)^{3/2} e^{-\frac{U_i}{k_B T}}\,, \tag{5}$$

where v is the plume velocity, $E = mne + mnv^2/2$ is the plume energy density, $e = (1 + \eta)(k_BT/m)/(\gamma - 1) + \eta U_i$ is the plume enthalpy, U_i is the ionization potential, u_+ and u_o are the electronic partition functions, m is the mass of the plume atom, m_e is the electron mass, h is Plank's constant, $S_n = n_{liq}v_{rs}$ is the density source, $S_E = n_{liq}v_{rs}k_BT_v/(\gamma - 1)$ is the energy source, n_{liq} is the liquid density, v_{rs} is the recession speed of the target surface due to ablation, and T_v is the vapor temperature. Here we take the small Knudsen layer limit, use $v = 0$ at the surface, and let S_n and S_E be constant. Because $c_s >> v_{rs}$, the surface recession on the plume expansion can be neglected (i.e., $x_s = 0$)[9].

3.1 A self-similar theory

For simplicity and comparision with the free expansion results, our analysis considers the gas to be neutral, which is a good approximation for $T_v \ll U_i$. With an energy source, the system is non-adiabatic near the surface. We expect self-similar expansion except for early times and a transition region near the surface (δx). The self-similar variable is $\xi \equiv x/v_m t$, where v_m is the maximum expansion velocity. We assume a velocity profile of $v = v_m[\alpha + (1-\alpha)\xi]$, where α is determined by the flow properties ($1 \geq \alpha \geq 0$). We transform the independent variables from (x, t) to ξ. From Eqs. (2) and (3) we obtain the density profile $n = n_\delta(1-\xi)^{(1-\alpha)/\alpha}$ and the pressure profile $P = n_\delta v_m^2 m\alpha^2(1-\alpha)/(1+\alpha)\,(1-\xi)^{(1+1/\alpha)}$; so the temperature profile is $k_BT/m = v_m^2\alpha^2(1-\alpha)/(1+\alpha)(1-\xi)^2$. From mass, momentum, and energy conservations, we know the relations of v_m, α, n_δ, and T_δ, which show the maximum expansion velocity scales as $1/\alpha$. The value $v_m/c_\delta = 4$ for $\alpha = 1/4$ corresponds to the case of adiabatic expansion with a Knudsen layer[6].

3.2 Numerical hydrodynamic modeling

The Rusanov scheme[10] is used to solve Euler's equations. Eqs. (2)-(4); the nonlinear calculation of T and η is done with the Newton-Raphson method[11]. We use the logarithm of Eq. (5) for numerical stability. The system size is 1,000 spatial grids, Δx. The initial adaptive size is 10^{-5} cm, which is required for numerical convergence. New vapor is added perturbatively into the first cell near the surface.

The typical physical parameters are as follows. The system is initiated with a uniform background gas with density $n_{bg} = 1 \times 10^{10}\,\mathrm{cm}^{-3}$ and temperature $T_{bg} = 293\,\mathrm{K}$. A constant source of vapor is specified for 6 ns with a temperature $T_v = 7000\,\mathrm{K}$, given by the Clausius-Clapeyron equation, and the target recession speed is $v_{rs} = 1 \times 10^3\,\mathrm{cm/s}$, which is typical for the ablation of silicon with laser fluence of a few $\mathrm{J/cm}^2$ [1]. We choose the mass of both source and background gas to be 28 a.m.u., a solid density of $5.01 \times 10^{22}\,\mathrm{cm}^{-3}$, an ionization potential of $1.3 \times 10^{11}\,\mathrm{erg}$ (8.1 eV), $u_+ = 6$, and $u_0 = 15$. We use $\gamma = 5/3$. Thus, $c_s = 1.85 \times 10^5\,\mathrm{cm/s}$. We note that the conventional free expansion model for no background gas (vacuum) gives a maximum expansion velocity of $5.55 \times 10^5\,\mathrm{cm/s}$.

We first study the case without the Saha equation (no ionization; i.e., $\eta = 0$). We check the profiles of density and velocity at $t = 5\,\mathrm{ns}$, at which time the expansion is almost steady state. From the simulations, we observe that the expansion develops self-similarly after 0.1 ns. The front position is at $x = 0.0069\,\mathrm{cm}$ at $t = 5\,\mathrm{ns}$. The maximum expansion velocity at this time is defined to be the ratio of the front position and the time; that is, $v_m = 1.38 \times 10^6\,\mathrm{cm/s}$ or $7.46\,c_s$. From the slope of the velocity profile, we estimate $\alpha = 1/14 = 0.07143$, which gives $v_\delta = 9.85 \times 10^4\,\mathrm{cm/s}$. Thus, $\delta x = 6.4 \times 10^{-5}\,\mathrm{cm}$. The simulation also shows that $n_\delta = 4.7 \times 10^{20}\,\mathrm{cm}^{-3}$ and $T_\delta = 3693\,\mathrm{K}$. The analytic profiles are given by $n = n_\delta(1 - x/0.0069\,\mathrm{cm})^{13}$ and $v = v_m/14 + (13/14)(x/5\,\mathrm{ns})$ from the self-similar theory. The analytic maximum expansion velocity is $7.42\,c_s$. Also, $n_\delta = 5.07 \times 10^{20}\,\mathrm{cm}^{-3}$ and $T_\delta = 2836\,\mathrm{K}$. The overall numerical profiles and scalings are in good agreement with the analytical theory. When we use the Saha equation (the more physical case), we find that the maximum velocity is about 40% higher. It reaches $1.70 \times 10^6\,\mathrm{cm/s}$ or $9.2\,c_s$ at $t = 10\,\mathrm{ns}$.

The higher maximum velocity is an effect due to dynamic partial ionization as a result of increased energy channeled into directed motion. This effect is reduced when the vapor temperature is lower; it gives only about a 6% increase when $T_v = 3500\,\mathrm{K}$, for example.

4. PLUME DYNAMICS IN BACKGROUND GAS

Laser ablation experiments have shown that the plume propagation in background gas can lead to the stopping of the ablated materials. In some cases the materials can even move backward, and several reflected shocks within the plume are apparent.

With the hydrodynamic modeling, we have simulated the plume dynamics with the following parameters: the recession speed of the solid silicon surface is 100 cm/s and lasts for 6 ns with a vapor temperature of 7000 K, and the background gas density is $6.6 \times 10^{15}\mathrm{cm}^{-3}$ at room temperature (i.e., the background pressure is 200 mTorr). Fig. 2 shows the plume dynamics at different times. At t = 10 ns as shown in Fig. 2(a), the background gas has been snowplowed. Also, the temperature and ionization fraction rise at the shock front. Fig. 2(b) shows that the relative higher pressure at the shock front has split the plume and background. This couples with the rarefaction of the plume to begin pushing the main body of the plume (second peak) backward and, thus, to slow it down. As a result, the velocity of the second peak is decreased toward zero. By t=100 μs, the velocity has become negative; that is, the second peak moves backward, as indcated in Fig. 2(c). The backward-moving plume eventually hits the target surface, rebounds, and moves forward again. The resultant plume splits, as shown in Fig. 2(d). We have also determined the scaling law for the turnover position of the ablated plume. The numerical modeling results show that the turnover position of the ablated plume is inversely proportional to the gas pressure and is proportional to the amount of ablated material.

5. SUMMARY

Both a thermal model for studying laser-solid interaction and a hydrodynamic model for the dynamics of laser-ablated materials have been developed. The thermal model shows that lower background pressure results in a lower laser-energy-density threshold for boiling, which

is consistent with experimental measurements. We have treated the laser-ablated material as a dynamic source, which is closer to experimental conditions, rather than as an initial constant source, as is done in free expansion models. It is demonstrated that the dynamic source and partial ionization effects can dramatically increase the front expansion velocity, which becomes significantly higher than predicted from a conventional free expansion model. For plume propagation in a background gas, our results show that the background gas acts on the main body of the rarefying plume, tending to slow it down, and in some cases even results in the backward movement of materials.

ACKNOWLEDGMENTS

This work is supported by the Oak Ridge National Laboratory (ORNL) Directed Research and Development Funds and the Division of Materials Sciences, U. S. Department of Energy, under contract DE-AC05-84OR21400 with Martin Marietta Energy Systems, Inc. K. R. Chen and C. L. Liu were supported in part by appointments to the ORNL Research Associate Program administered jointly by the Oak Ridge Institute for Science and Education and ORNL.

References

[1] R. F. Wood and G. A. Geist, *Phys. Rev. Lett.* 57, 873 (1986).

[2] G. E. Jellison, Jr., D. H. Lowndes, D. N. Mashburn, and R. F. Wood, *Phys. Rev. B* 34, 2407 (1986).

[3] D. H. Lowndes, *et. al.*, *Appl. Phys. Lett.* 41, 938 (1982).

[4] D. B. Chrisey and G. K. Hubler, *Pulsed Laser Deposition of Thin Films*, John Wiley & Sons:New York (1994).

[5] L. D. Landau and E. M. Lifshitz, *Fluid Mechanics*, Addison-Wesley:New York, 357 (1959).

[6] R. Kelly, *J. of Chem. Phys.* 92, 5047 (1990) and references therein.

[7] R. Kelly, A. Miotello, A. Mele, A. Giardini, J. W. Hastie, P. K. Schenck, and H. Okabe, submitted to *Surf. Sci.* Also, private communication with R. Kelly.

[8] See, for example, A. Vertes, in *2nd Int'l Conf. on Laser Ablation: Mechanisms and Application-II*, edited by J. C. Miller and D. B. Geohegan, AIP Conf. Proc. No. 288, 275 (1994).

[9] G. Weyl, A. Pirri, and R. Root, *AIAA J.* 19, 460 (1981).

[10] G. A. Sod, *J. of Comput. Phys.* 27, 1-31 (1978).

[11] W. H. Press, B. P. Flannery, S. A. Teukolsky, and W. T. Vetterling, *Numerical Recipes (FORTRAN Version)*, 267 (1989).

Figure Captions

Fig.1. Laser-energy-density threshold(circle) and vaporization temperature(square) vs. pressure.

Fig.2. The profiles of density, pressure, and velocity vs. position at different times: (a) t = 10 ns, (b) t = 1 μs, (c) t = 100 μs, and (d) t = 500 μs.

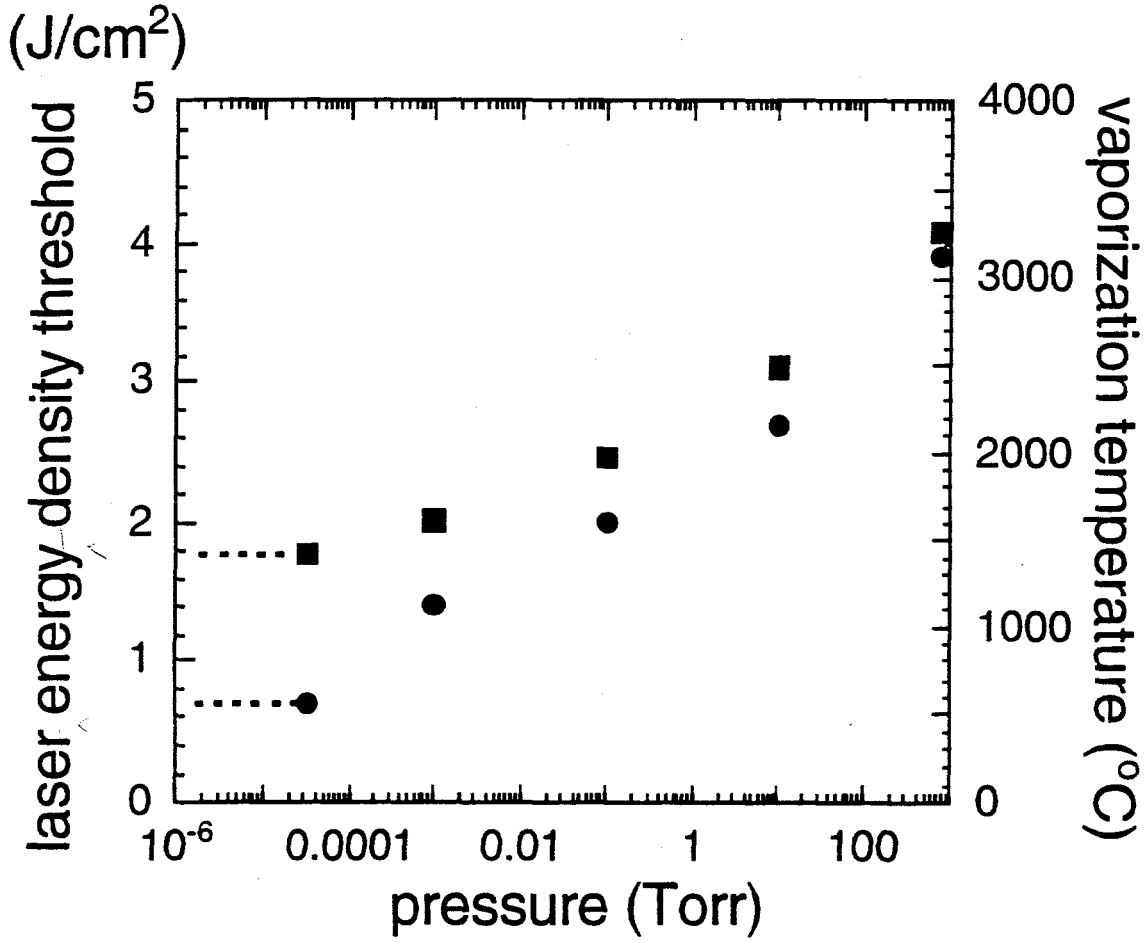

Fig.1 by Chen, et al.

(a)

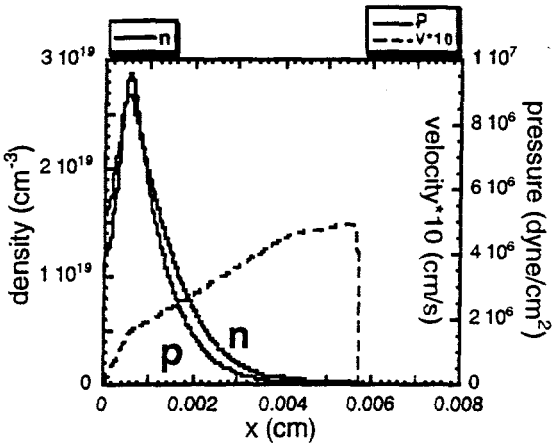

(b)

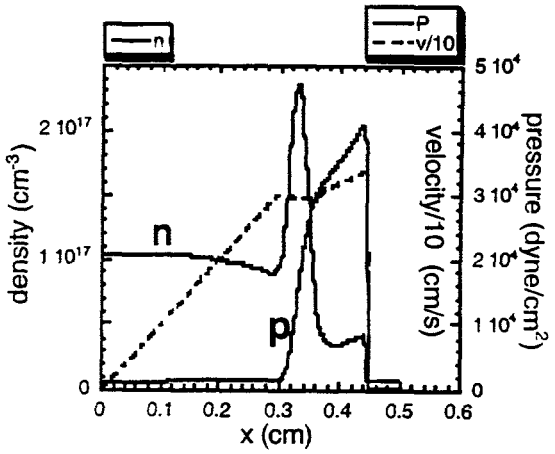

(c)

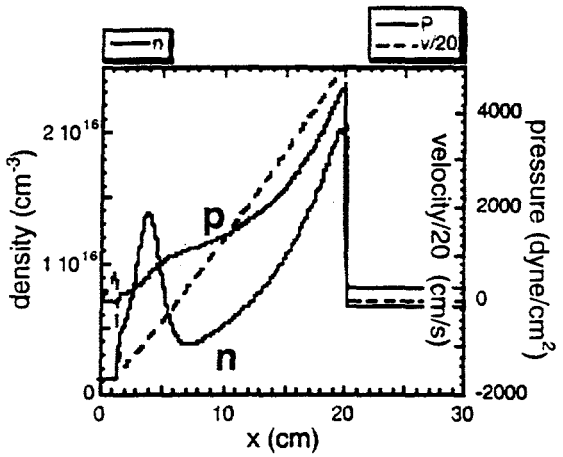

(d)

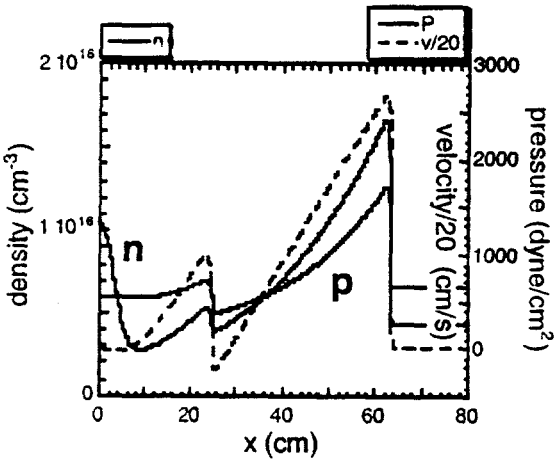

Fig. 2 by Chen, et al.